UNIVERSIDADE D
COIMBRA

José Pedro Silva Pereira

Matrix Based Implementation of Time-Interleaved Block Windowed Burst OFDM

Dissertação no âmbito do Mestrado Integrado em Engenharia Eletrotécnica e de Computadores, no ramo de especialização de Telecomunicações, orientada pelo Professor Doutor Marco Alexandre Cravo Gomes e pelo Professor Doutor Vitor Manuel Mendes da Silva e apresentada ao Departamento de Engenharia Eletrotécnica e de Computadores da Faculdade de Ciências e Tecnologia da Universidade de Coimbra

Outubro de 2021

This page intentionally left blank.

1 2  9 0 UNIVERSIDADE D COIMBRA

Matrix-based implementation of Time-Interleaved Block Windowed Burst OFDM

José Pedro Silva Pereira

Dissertação para obtenção do Grau de Mestre em

Engenharia Electrotécnica e de Computadores

Orientada por: Doutor Marco Alexandre Cravo Gomes
Doutor Vitor Manuel Mendes da Silva

Júri

Presidente: Doutor Luís Alberto da Silva Cruz
Orientador: Doutor Marco Alexandre Cravo Gomes
Vogal: Doutor Lúcia Maria dos Reis Albuquerque Martins

Outubro de 2021

This page intentionally left blank.

”Community is everything… you can’t change the world, but you can make a corner of it pretty nice”

- Dave Chappelle

This page intentionally left blank.

Agradecimentos

Em primeiro lugar, agradecer aos meus orientadores, Prof. Dr. Marco Gomes e Prof. Dr. Vítor Silva por todo o apoio, profissionalismo e paciência ao longo desta dissertação. Obrigado pela motivação e pela constante disponibilidade.

Ao Instituto de Telecomunicações pelos recursos disponibilizados, métodos de trabalho e pelo ambiente acolhedor.

Aos meus pais, por me acompanharem em mais uma etapa da vida, com o apoio e carinho de sempre. Obrigado por me darem a melhor escola da vida que uma pessoa poderia ter e por serem um grande exemplo em qualquer circunstância. Não posso deixar de dizer que estou grato ao Stand Jucar por nunca me recusar boleia ao longo desta longa caminhada.

Aos Kappa, Berto, Luis, Guido e Rui, por tornarem noites normais de jogo em grandes aventuras de riseira infinita. Ainda temos de ir a Paris tratar das cáries e ao Bubbles!

Aos meus amigos dos AIF, por todas os convívios e fins de semana. Ia escrever os vossos nomes todos, mas o documento tem limite de páginas! Silvares, Bouças e Lameira estarão sempre no meu coração.

Ao NEEEC/AAC por me ter ensinado o significado de espírito de equipa, entre-ajuda e sacrifício. Ao Steve e Gertrudes que me puseram o bichinho da Administração. Um especial obrigado ao Bento, Ivo e Miguel pelas reuniões longas que me tiraram anos de vida, mas que deram azo a uma equipa e uma estrutura nunca antes tão bem organizada.

Ao 1º esquerdo, por todas as experiências e companheirismo, ao Dinis, Jorge, Luca e Tiago. Um especial obrigado ao Marco Silva por tornar a quarentena menos longa e por toda a ajuda e soluções para tudo.

Ao pessoal de Telecomunicações, que sempre mostrou grande espírito de camaradagem, ao Mário, Gonçalo, Zé Chico e Lemos.

A todos os meus grandes amigos que a cidade dos Estudantes me deu: ao Moisés, Baltazar, Henriques e Rui Gouveia. Ao João Martins por todo o apoio, motivação e aventuras durante o meu percurso. Espero que um dia consigas pagar as boleias todas!

À Filipa por me acompanhar nesta caminhada e me ajudar sempre a ser racional nos momentos mais confusos. Obrigado por tornares tudo mais fácil.

A todos,
Muito Obrigado!

Este trabalho foi financiado pela FCT/MEC atraves de fundos nacionais e quando aplicável co-financiado pelo FEDER - PT2020 no âmbito do projeto UIDB/50008/2020-UIDP/50008/2020 e PES3N (2018-SAICT-45-2017-POCI-01-0145-FEDER-030629) e MASSIVE5G(POCI-01-0145-FEDER-030588).

This page intentionally left blank.

Abstract

We live in an era where the world of communications is becoming increasingly demanding, as technology around it evolves. Hence, it is crucial to understand and overcome all the demands that the upcoming generation of wireless networks require. One of the most important aspects is to maintain low complexity systems, that are capable enough of granting high spectral efficiency, under adverse channel conditions.

The Orthogonal Frequency Division Multiplexing (OFDM) has been the modulation technique of reference for 4G systems, considering that it provides high data transmission rates and it is based on the Fast Fourier Transform (FFT) and the Inverse Fast Fourier Transform (IFFT), which allows low complexity systems. In an OFDM transmitter, the high data rate stream is divided into N parallel lower rate streams, the sub-carriers, that are orthogonal to each other. This orthogonality between the sub-carriers grants a robustness against Inter Carrier Interference. Nonetheless, this approach still has some drawbacks, such as a limited spectral and power efficiencies. Thus, in order to deal with these issues, new hybrid modulation techniques were developed, such as the Time Interleaved Block Windowed Burst OFDM (TIBWB-OFDM).

The TIBWB-OFDM architecture allows the transmitted signal to be resilient to deep in-band fades, as the information is replicated through the entire channel's bandwidth. Additionally, it uses a smoother window than the conventional OFDM, a Square Root Raised Cosine one. However, the spectral efficiency of the TIBWB-OFDM is still limited by the increased length of its blocks, in time domain. This issue can be tackled by using a different packing approach for the TIBWB-OFDM symbols, by using Windowing Time Overlapping (WTO), which allows the windowed OFDM blocks to be partially overlapped in time.

Therefore, this dissertation proposes a parallelization of TIBWB-OFDM by implementing

a computational efficient matrix framework of the TIBWB-OFDM with WTO transceiver.

Keywords

Time Interleaved Block Windowed Burst OFDM with Windowing Time Overlapping (TIBWB-OFDM with WTO), Frequency Domain Equalization (FDE), Matrix Framework, Spectral Efficiency, Parallelization

Resumo

Vivemos numa era onde o mundo das comunicações se está a tornar cada vez mais exigente, à medida que a tecnologia evolui. Portanto, é fundamental compreender e superar todos os desafios que as próximas gerações de redes sem fios exigem. Um dos aspetos mais importantes é manter a baixa complexidade dos sistemas, mas que sejam capazes de garantir alta eficiência espetral em condições adversas de canal.

O *Orthogonal Frequency Division Multiplexing (OFDM)* tem sido a técnica de modulação de referência para sistemas 4G, dado que permite altas taxas de transmissão de dados e é baseado na transformada de Fourier rápida (FFT) e a sua inversa (IFFT), que permite manter a baixa complexidade dos sistemas. Num transmissor OFDM, os dados com alta taxa de transmissão são divididos em N sub-portadoras de ritmo inferior, que são ortogonais entre si. Esta ortogonalidade, entre as sub-portadoras, garante uma robustez contra Interferência Inter Canal (ICI). No entanto, esta abordagem possui algumas limitações, sendo as principais uma limitada eficiência espetral e energética. Assim, para lidar com esses problemas, foram desenvolvidas novas técnicas de modulação híbrida, como o *Time Interleaved Block Windowed Burst OFDM (TIBWB-OFDM)*.

A arquitetura do TIBWB-OFDM permite que o sinal transmitido seja resiliente a desvanecimentos de banda profundos (*deep in-band fades*), uma vez que a informação é replicada ao longo de toda a largura de banda do canal. Para além disso, é usada uma janela mais suave que a do OFDM convencional, a janela *Square Root Raised Cosine (SRRC)*. Porém, o TIBWB-OFDM também apresenta uma eficiência espetral limitada à medida que o comprimento dos seus blocos (no domínio do tempo) aumenta. Esta contrariedade pode ser colmatada usando uma abordagem diferente para a compactação dos símbolos TIBWB-OFDM, que permite que os blocos OFDM janelados sejam parcialmente sobrepostos - TIBWB-OFDM com *Windowing Time Overlapping (WTO)*.

Portanto, esta dissertação propõe uma paralelização do TIBWB-OFDM ao implementar

uma versão matricial eficiente do transcetor TIBWB-OFDM com WTO.

Palavras Chave

Time Interleaved Block Windowed Burst OFDM with Windowing Time Overlapping (TIBWB-OFDM with WTO), Igualização no Domínio da Frequência, Estrutra matricial, Eficiência Espetral, Paralelização

Contents

List of Figures

This page intentionally left blank.

List of Acronyms

3GPP 3rd Generation Partnership Project

ADC Analogue-to-Digital Converter

AWGN Aditive White Gaussian Noise

BWB Block Windowed Burst OFDM

BER Bit Error Rate

BS Base Station

CP Cyclic Prefix

DFT Discrete Fourier Transform

DAC Digital-to-Analogue Converter

EGC Equal Gain Combiner

FFT Fast Fourier Transform

FDE Frequency Domain Equalization

FF Feedfoward

FB Feedback

ICI Inter Carrier Interference

ISI Inter Symbol Interference

IBI Inter Block Interference

IFFT Inverse Fast Fourier Transform

IDFT Inverse Discrete Fourier Transform

IB-DFE Iterative Block Decision Feedback Equalization

LLR Log-likelihood ratio

LoS Line of Sight

MIMO Multiple-Input Multiple-Output

MMSE Minimum Mean Square Error

MC Multi-Carrier

MRC Maximum Rate Combiner

OFDM Orthogonal Frequency Division Multiplexing

OOB Out-Of-Band

PAPR Peak-to-Average Power Ratio

PSD Power Spectral Density

QPSK Quadrature Phase Shift Keying

SRRC Square Root Raised Cosine

SDR Software Defined Radio

SNR Signal-to-Noise Ratio

SISO Single-Input Single-Output

SC Single Carrier

S/P Serial to Paralel

SU Single-User

TDE Time Domain Equalizer

TIBWB Time Interleaved Block Windowed Burst OFDM

USRP Universal Software Radio Peripheral

WTO Windowing Time Overlapping

ZF Zero-Forcing

ZP Zero-Padding

1

Introduction

Contents

The world of mobile communications is becoming increasingly demanding, as technology around it evolves. So, there is an urgent need to understand and overcome all the challenges that the next generation of communications entail. This means that, while maintaining a high spectral efficiency, these services and their respective networks should be robust and deliver very low latencies, while performing under unfavourable channel conditions.

1.1 Motivation and Context

Orthogonal Frequency Division Multiplexing (OFDM) has been the modulation technique of reference for 4G systems and considered, by 3GPP, for 5G [7], since it allows low complexity systems, based on the Fast Fourier Transform (FFT) and the Inverse Fast Fourier Transform (IFFT), to get a high and robust data transmission rate. OFDM is a Multi-Carrier (MC) approach that splits a high rate data stream into N parallel lower rate streams [4] - the sub-carriers, which are orthogonal to each other. Such fact allows OFDM systems to avoid Inter Carrier Interference (ICI) and to have a simple Frequency Domain Equalization (FDE), as long as the Cyclic Prefix (CP) is greater than the channel delay spread [8].

Although OFDM favors the equalization process and the use of relatively simple equalizers, it has its drawbacks, being the main one a limited spectral and power efficiency. This results in the need to use linear power amplifiers (that have low efficiency) capable of ensuring a distortion-free amplified signal, which is very hard to warrant. As an alternative to this, Block Windowed Burst OFDM (BWB-OFDM) was developed to cover some of the OFDM issues by using a Zero-Padding (ZP) guard interval, instead of the conventional Cyclic Prefix (CP), and a smoother and non-rectangular window (SRRC) window, which grants a better spectrum confinement [9]. Still, both OFDM and BWB-OFDM performances can be disturbed by the deep fade regions of time-dispersive channels.

As a complement and improvement to both OFDM and BWB-OFDM, Time Interleaved Block Windowed Burst OFDM (TIBWB-OFDM) was developed and will be of particular interest throughout this work. This new hybrid modulation technique reduces the harm caused by the deep fading events through the replication of the information all over the designated bandwidth. Additionally, TIBWB-OFDM offers higher transmission rates and increased energy efficiency of the overall communication system [6].

1.2 Objectives

The most significant purpose of this dissertation is to present a new and more efficient TIBWB-OFDM transceiver, more specifically when employing Windowing Time Overlapping (WTO). Although the overlapping process smooths the waveform, which reduces the windowing attenuation, it also corrupts the data of adjacent sub-blocks. Therefore, it is crucial to develop techniques to properly equalize and reconstruct the TIBWB-OFDM received signal, in time domain. Focusing on such goal, a backward and forward cancellation method is presented in this work, based on a efficient matrix process, which aims to efficiently recover the once corrupted overlapped data, with fast and straightforward computations, that can be easily parallelized.

1.3 Dissertation outline

This dissertation is divided into four chapters. The current chapter provides the motivations and objectives of this work. Chapter 2 presents the research background, exposing SC and MC techniques, emphasizing OFDM, while Chapter 3 displays the new hybrid BWB-OFDM methods. In Chapter 4 the new TIBWB-OFDM with WTO algorithm is introduced, along with the new matrix version of it. Chapter 5 discusses the obtained results and the respective conclusions.

This page intentionally left blank.

2

Background

Contents

This chapter presents some relevant scientific research, regarding the SC and MC modulation techniques and how they are employed throughout this work.

2.1 Wireless Propagation

Wireless communications offer a wide range of possibilities, such as its mobility and flexibility, while being easily installed and relatively cheaper than wired networks. However, a wireless channel cannot be designed and optimised in the same way that a transmitter or receiver can. Thus, bearing in mind that a transmitted wireless signal suffers changes throughout its propagation path, before arriving at its receiver, it is crucial to consider two unavoidable factors when engineering a wireless system: large-scale fading and small-scale fading [10].

Large-scale fading is induced by signal attenuation caused by long distance transmission and diffraction around large obstacles in the propagation path. It is provoked by both path loss (P) and shadowing (S). In a Line of Sight (LoS) free space transmission the attenuation of a given wireless signal obeys the $\frac{1}{d^2}$ distance law [11]. However, in a real scenario there is generally no straight LoS path linking mobile stations with the base station. Supposing that there is a direct LoS between the transmitting antenna (Tx) and a receiving antenna (Rx), the path loss relates with the received signal power, $P_r(d)$, and the distance d, between the two antennas:

$$P_r(d) \propto \left(\frac{\lambda}{4\pi d}\right)^2 \tag{2.1}$$

where λ is the wavelength of the carrier signal. Thus, through a free space propagation, the received power by Rx decreases proportionally to the the square of d, the distance between Tx and Rx. Furthermore, as the frequency of the carrier increases, the path loss also increases, since the frequency, f, is inversely proportional to the wavelength, λ.

Small-scale fading is defined by abrupt changes in the received signal strength over a relatively short distance and time period [11]. Such variations happen due to multi-path fading, created by small obstacles that cause reflection, diffraction and/or scattering. As a result, the signal is received with delay spread, which can be seen as distinct signal echoes arriving at different times. Thus, the impulse response of a time-varying channel, $h(\tau;t)$, can be represented by:

$$h(\tau;t) = \sum_i \alpha(t) e^{-j\theta_i(t)} \delta(\tau - \tau_I) \tag{2.2}$$

with $\alpha(t)$ is the complex amplitude, $\delta(\tau)$ the Dirac delta function and τ_i the delay of the *i-th* path.

2.2 SC and MC modulation techniques

In a Single Carrier (SC) modulation system only a signal frequency is used to transmit the desired data. Hence, considering the system transmission rate as R_S, the occupied bandwidth

is, at least, $B = \frac{R_S}{2}$. Typically, wireless channels are frequency selective and characterized by a given coherence bandwidth, B_c. Coherence bandwidth is a measure of the frequency range over which the frequency response of the channel can be considered flat. So, if B is much higher than B_c, in time dispersive channels, fading is likely to occur. Additionally, considering the fact that the currently used and upcoming transceivers must handle high data transmission rates, SC systems cause a huge delay spread, higher than the symbol duration, which creates ISI.

Since it is really challenging to avoid ISI using SC modulation, due to its need of complex systems, Multi-Carrier (MC) transmission was introduced. The principle of this method is to divide the data stream into N several ones, which allows each stream to have a lower bit rate, given by $\frac{R_S}{N}$. This prevents ISI, given that the symbol duration is much larger than the delay spread, and keeps the channel equalization and estimation a less painless process [12]. Still, it is necessary to deal with potential ICI, if, for instance, the sub-carriers frequencies are near to one another. By including a guard interval between each sub-channel this issue can be eliminated, although some spectral efficiency is lost.

2.3 Orthogonal Frequency Division Multiplexing

OFDM is one of the most prominent digital MC modulation techniques, since it expanded the use of a single sub-carrier modulation by using N lower rate sub-carriers within the same single channel.

An OFDM signal is represented by N contiguous and orthogonal sub-carriers that are evenly spaced, at frequency domain, by $\frac{1}{NT_s}$, where $\frac{1}{T_s}$ is the transmission rate [12]. In an OFDM scheme, a bit-stream is first mapped into a chosen $M-ary$ signal constellation and then channel-coded and bit-interleaved. The generated complex numbers are then subjected to a serial to parallel S/P conversion and the pilot symbols are attached into the OFDM signal. In order to avoid ISI, a CP is inserted across each block after the IFFT process is applied [13]. OFDM can be easily implemented, based on DFT and IDFT, in low complex systems, allowing a fast and efficient computation of both FFT and IFFT, respectively. Hence, an OFDM transmitted signal, $s[n]$, can be expressed as follows:

$$\mathbf{s} = [s_n]_{n=0,\cdots,N-1} \quad \text{and} \quad s_n = \sum_{k=0}^{N-1} S_k e^{\frac{j2\pi nk}{N}}, n = 0,\ldots,N-1 \tag{2.3}$$

where S_k is the symbol of the M-ary constellation transmitted at the carrier k. Since T_S indicates the symbol duration, NT_s represents the entire OFDM block duration.

On the OFDM receiver, the CP is removed and the obtained signal, y_n, is converted into frequency domain and equalized, resulting in $\widetilde{S}_k$. Then, to acquire the estimated bit-stream, $\widetilde{b}$, the symbol sequence must go through demapping, bit-deinterleaving and channel decoding processes. OFDM is quite robust to ICI, due to its sub-carriers orthogonality, allowing the receiver to decode the OFDM signal in a straightforward manner.

2.3.1 Downsides of OFDM

Regardless of being such a developed technique, OFDM still has its drawbacks, namely its limited spectral and power efficiency. Since ISI may happen as a result of varying temporal delays during reception, a guard interval, at the start of each symbol, is required. Considering this guard interval as CP, a CP-OFDM system has a total signal length of $N_{CP-OFDM} = N_{CP} + N$ [14]. The CP size is given by N_{CP} and it has to be larger than the channel delay spread, so that ISI can be eliminated. Consequently, the use of a guard interval, although being crucial, it comes with a reduction of the overall spectral efficiency of the system.

Additionally, is it mandatory that both the OFDM transmitter and receiver have the same sampling frequency, due to the fact that this technique is highly sensible to synchronization errors. For instance, if there is a slight frequency offset, the orthogonality of the sub-carriers can be ruined, which causes ICI [13].

Another issue regarding OFDM systems is the windowing configuration. An OFDM symbol windowed by a unitary rectangular window, $w[n]$, can be represented through:

$$s_n = s[n] = \sum_{k=0}^{N-1} S_k W[n] e^{\frac{j2\pi nk}{N}}, n = 0, ..., N-1 \tag{2.4}$$

where S_k is the symbol of the M-ary constellation transmitted at the carrier. The spectrum of this rectangular pulse is a *sinc*, which means that its abrupt transitions, at the time domain, causes the high amplitude OFDM spectrum to be assigned outside of its bandwidth. As a result, the lateral spectral side lobes can cause Out-Of-Band (OOB) emissions, lowering the global spectral efficiency of the system.

The high Peak-to-Average Power Ratio (PAPR), rised by the considerable peaks of the OFDM signal's envelope, causes a decrease in the amplification efficiency [15]. The PAPR of a time-continuous signal, $x(t)$, is given by:

$$PAPR = \frac{max\,|x(t)|^2}{E\left\{|x(t))|^2\right\}} \Leftrightarrow 10log_{10}\left(\frac{max\,[x(t)x^*(t)]}{E\,[x(t)x^*(t)]}\right)[dB] \tag{2.5}$$

where $x^*(t)$ represents the conjugate of $x(t)$ and $E[]$ the mean value. As the number of OFDM subcarriers increases, the PAPR also increases. Because of this high PAPR level, the transmitter's power amplifier must have a wide dynamic range, which significantly decreases its efficiency [15].

3

OFDM-based Hybrid Modulation Techniques

Contents

This chapter covers the key theoretical concepts of both BWB-OFDM and TIBWB-OFDM, the hybrid modulation techniques employed throughout this work.

3.1 Block Windowed Burst OFDM (BWB-OFDM)

Aiming to achieve a higher spectral and power efficiency than the conventional Orthogonal Frequency Division Multiplexing scheme, whilst maintaining high transmission data rates, the Block Windowed Burst OFDM [16] modulation technique was proposed. The main feature of BWB-OFDM is removing of CP without giving in systems' low complexity and its advantages.

Based on the OFDM transmitter, the BWB-OFDM symbol packs N_s OFDM symbols. As in conventional OFDM the bit-stream, b, is first channel-coded and bit interleaved,so that the BER performance is improved. Then, this sequence is mapped om a M-ary constellation. Afterwards, the high data stream is split into $N_s \times N$ lower rate sub-streams and N_s OFDM symbols with size N are obtained. To each of the individual conventional OFDM symbols, $\mathbf{s}_i$, with $i = 1,...,N_s$, given by (2.4) is then applied a window operation, by using a smoother Square Root Raised Cosine (SRRC) window [12]:

$$h_{SRRC}[n] = \begin{cases} 1 & ,|n| < \frac{N}{2}(1-\beta) \\ cos(\frac{\pi}{4\beta}\left[\frac{2n}{N} - (1-\beta)\right]), & \frac{N}{2}(1-\beta) \leq |n| \leq \frac{N}{2}(1+\beta) \\ 0 & ,|n| \geq \frac{N}{2}(1+\beta) \end{cases} \tag{3.1}$$

where $n = -N,...,N$ and β is the window roll off value that grants an improved spectral efficiency, by attenuating the secondary lobes. Each resulting windowed symbol, $\mathbf{s}_{w,n}$, can be mathematically represented by:

$$\mathbf{s}_{w,n} = [\mathbf{s}_n|\mathbf{s}_n]_{(1X2N)} \odot \mathbf{h}_{SRRC_{(1x2N)}} \tag{3.2}$$

where $\odot$ represents a point-wise product and the bold label a vector. The figure below compares the two windowing techniques, concerning their Power Spectral Density (PSD) disparities:

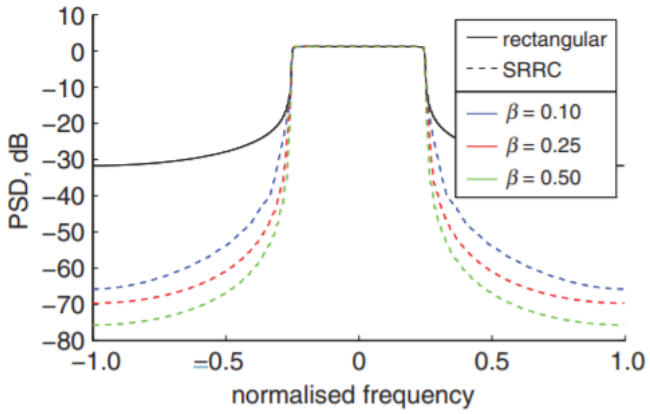

Figure 3.1: PSD of the windowed signal with a SRRC window in time domain [1]

The BWB-OFDM frame is then formed by packing those N_s symbols together, $s_{w,n}$:

$$\mathbf{s}_B = [\mathbf{s}_{w,1}|\mathbf{s}_{w,2}|...|\mathbf{s}_{w,N_s}]_{(1\times N_b)} \tag{3.3}$$

where $N_b = N_s \times N(1+\beta)$. At the BWB-OFDM symbol is added a single ZP guard interval, instead of the conventional CP, and it can be expressed by:

$$\mathbf{x}_n = \left[\mathbf{s}_B|0_{(1\times N_{ZP})}\right]_{(1\times N_x)} \tag{3.4}$$

where N_{ZP} corresponds to the null ZP added samples and $N_x = N_S \times N(1+\beta)+N_{ZP}$.

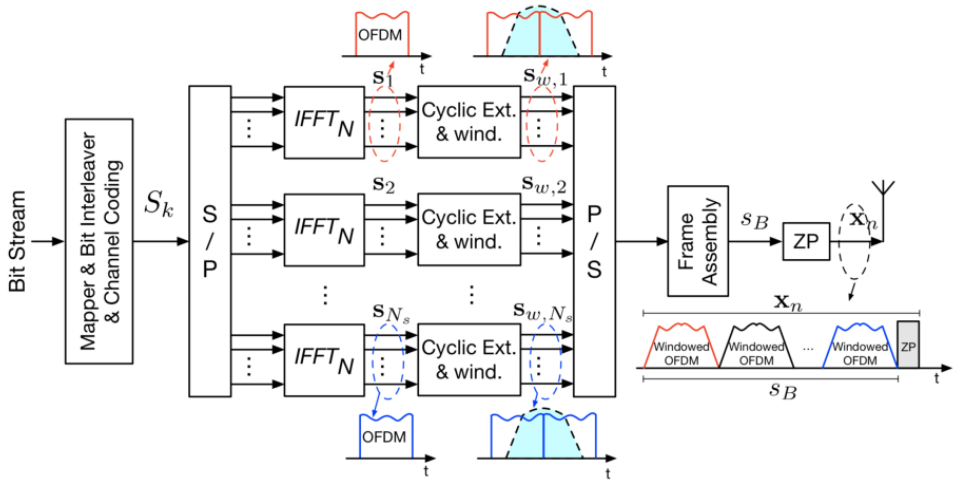

Figure 3.2: BWB-OFDM transmitter scheme outline [2]

On the BWB-OFDM decoder presented on figure 3.3, the received BWB-OFDM block, $\mathbf{y}_n$, is equalized in frequency domain as a whole, resulting in the estimated block, $\hat{\mathbf{X}}_k$. After-

wards it is converted into time domain, $\hat{\mathbf{x}}_n = IDFT(\hat{X}_k)$ and the ZP guard interval is withdrawn. The same windowing process is applied (matched filtering) after adding sufficient null samples capable of increasing the length of symbol until $2N$:

$$\hat{s}_{w,j} = \hat{x}_{n,j_{(1\times 2N)}} \odot h_{SRRC_{(1\times 2N)}} \tag{3.5}$$

These $\hat{\mathbf{s}}_{w,j}$ BWB-OFDM symbols are then converted into frequency domain and down sampled by 2, acquiring the $\mathbf{S_k}$ estimated OFDM data. Lastly, the channel decoding and bit-deinterleaving operations are carried out.

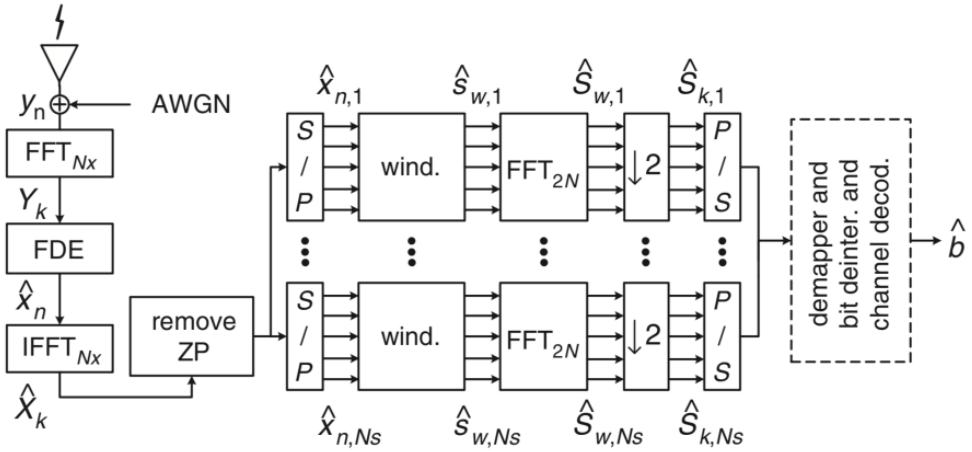

Figure 3.3: BWB-OFDM receiver scheme outline [1]

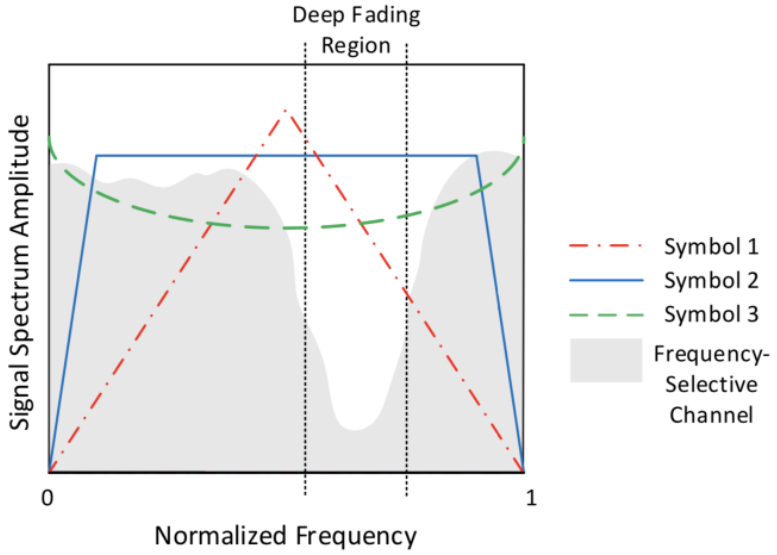

Figure 3.4: BWB-OFDM symbol's amplitude spectrum [3]

Comparing to OFDM, BWB-OFDM offers a better spectral confinement and a higher bit

rate, although it has some drawbacks too, such as poor performance in hostile channel conditions. This happens when a set of sub-carriers of the several OFDM symbols, packed in the BWB-OFDM block, are affected by deep fade zones, as seen in figure 3.4 [16]. As a result, the BWB-OFDM receiver might have issues in retrieving the transmitted signal, if the desired spectral data is located on those fading regions, decreasing the overall system performance.

3.2 Time Interleaved Block Windowed Burst OFDM

The TIBWB-OFDM transmitter grows from the BWB-OFDM one, although it allows the signal to be resilient to deep in-band fades without compromising the low complexity shown in BWB-OFDM systems. This aims not only to keep the good spectral efficiency characteristics of BWB-OFDM, but also to broaden its robustness against the dispersive channel effects [16]. Hence, the principle of TIBWB-OFDM is to replicate the information through all the channel's bandwidth by expanding each OFDM symbol that compose the BWB-OFDM block in time by a factor N_s. Figure 3.5 depicts that process for $N_s = 3$:

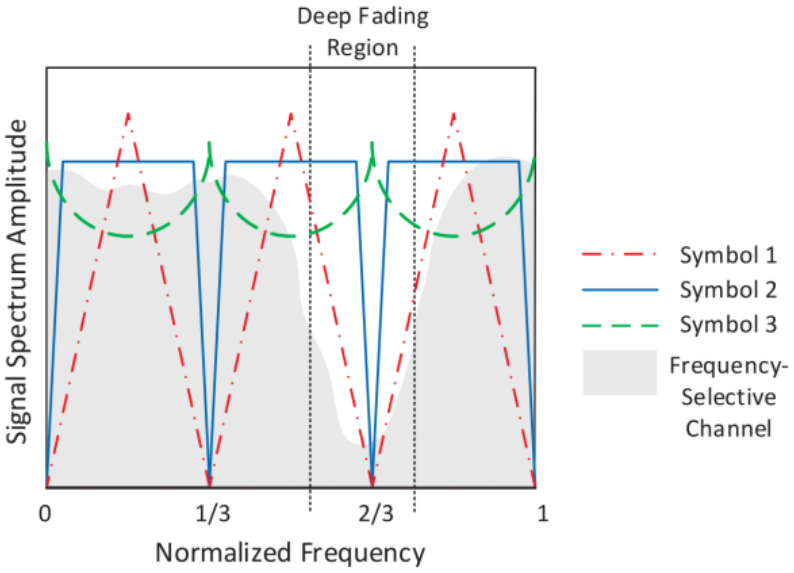

Figure 3.5: TIBWB-OFDM signal amplitude spectrum formed by 3 OFDM symbols [3]

As the TIBWB-OFDM transmitter reproduces the data several times in other parts of the spectrum, the corrupted information can be easily retrieved, making the effect of the deep fade regions less problematic.

Figure 3.6 details the construction of the TIBWB-OFDM block. The first stages of TIBWB-OFDM transmission are the same as the BWB-OFDM, until the construction of vector $\mathbf{s}_B$ given by (3.4). After those operations a time-interleaver is applied and the block vector is generated by:

$$\mathbf{s}_\pi = \mathbf{s}_b \prod(N_s) \tag{3.6}$$

where $\prod(N_s)$ is the $[N_b \times N_b]$ periodic interleaving matrix with period N_s. Lastly, the guard interval ZP is added at the end of the block, so that the transmitted TIBWB-OFDM symbol can deal with frequency selective multi-path channel's delay spread:

$$\mathbf{x}_n = [s_\pi | 0_{1\times N_{ZP}}]_{1\times N_x} \tag{3.7}$$

where $\mathbf{x}_n$ has length $N_x = N_S \times N(1+\beta) + N_{ZP}$.

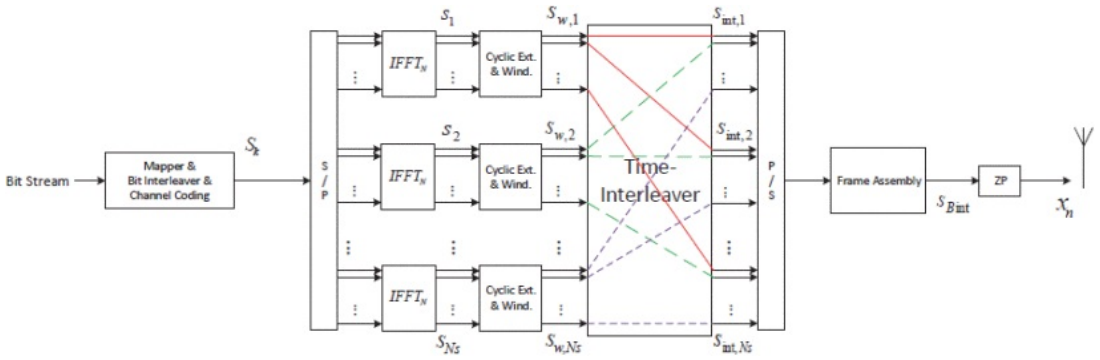

Figure 3.6: TIBWB-OFDM transmitter design [3]

The TIBWB-OFDM receiver main objectives are to equalize the received signal, perform deinterleaving and match filtering, in order to compensate carrier impairments and avoid ICI before the demodulation and channel decoding. Through a N_x sized DFT, the received signal, y_n, is converted to the frequency domain, Y_k:

$$Y_k = X_k H_k + \eta_k \qquad ,k = 0,...,N_{x-1} \tag{3.8}$$

where H_k is the channel impulse response and η_k is Aditive White Gaussian Noise (AWGN), $X_k = DFT(x_n)$ and $k = 0,1,...,N_x - 1$. Afterwards, the the TIBWB-OFDM signal is estimated using linear Frequency Domain Equalization, expressed by:

$$\hat{X_k} = F_K Y_k \tag{3.9}$$

Then, $\hat{X_k}$ is converted back to the time domain and the guard interval (ZP) is removed from the TIBWB-OFDM block, followed by time-deinterleaving. The same SRRC window used in the transmitter is applied to each sub-block (matched-filtering), and a few number of zeros is added to each symbol until its dimension is $2N$:

$$\hat{s}_{w_i} = \hat{x}_{n_i} \odot \mathbf{h}_{\mathbf{SRRC}(1\times 2N)} \tag{3.10}$$

Finally, the estimation of the initial transmitted symbol is obtained by applying a $2N$ FFT and down-sampling it by 2. The channel decoding, demapping and bit-deinterleaving operations are then carried out.

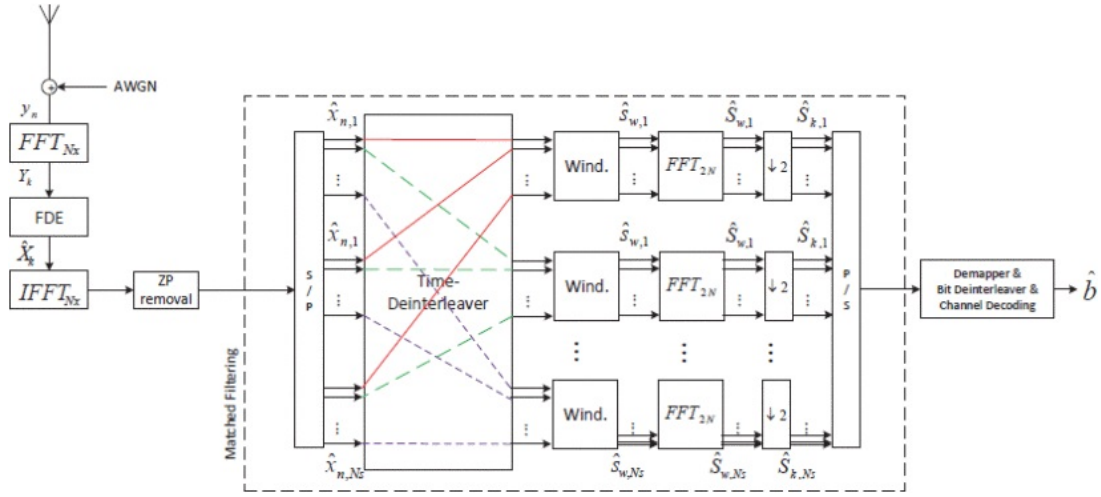

Figure 3.7: TIBWB-OFDM receiver design [3]

3.3 TIBWB-OFDM with Iterative Block Decision Feedback Equalization

Despite the fact that the FDE addressed in the previous section perform quite well, there is room for improvement. Hence, the Iterative Block Decision Feedback Equalization (IB-DFE) equalizers emerged as a more advanced way to deal with both Inter Block Interference (IBI) and ISI, by using two relevant filters: **(1)** the Feedforward (FF) filter (F_k^l), similar to a conventional linear FDE that deals with the precursors created by the channel and **(2)** the Feedback (FB) filter (B_k^l), which tries to eliminate ISI and IBI using data from a previous estimation [3].

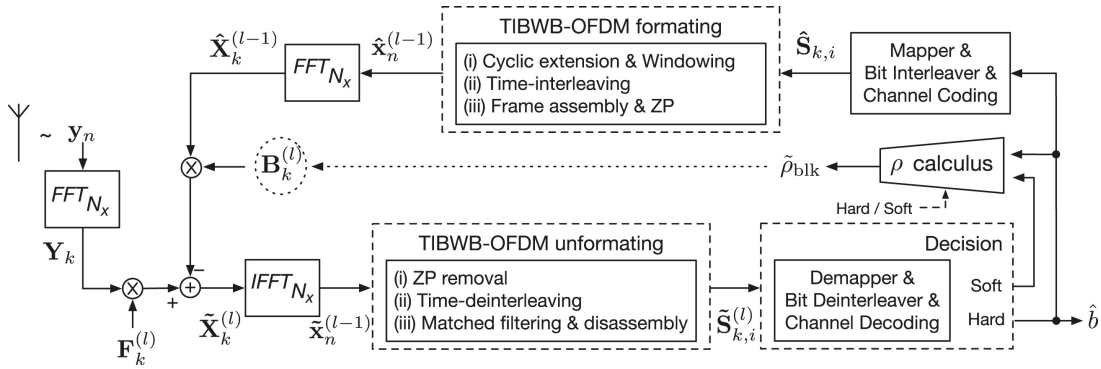

Figure 3.8: Turbo IB-DFE design for the TIBWB-OFDM receiver [1]

The TIBWB-OFDM with IB-DFE is shown in figure 3.8, where the received signal, Y_k, is processed by the equalizer, resulting in a block that acts as a estimation of the TIBWB-OFDM symbol, $\widetilde{X}_k^{(l)}$, for each iteration l, which is given by:

$$\widetilde{X}_k^{(l)} = F_k^{(l)} Y_k - B_k^{(l)} \widetilde{X}_k^{(l-1)} \tag{3.11}$$

where $F_k^{(l)}$ and $B_k^{(l)}$ are the FF and FB filter coefficients, executing either *soft* or *hard decisions*. The optimal values for these coefficients are, respectively [3]:

$$F_k^{(l)} = \frac{\kappa H_k^*}{\frac{1}{\gamma} + (1 - \rho_{blk}^{(l-1)} |H_k|^2)} \tag{3.12}$$

for the FF filter and

$$B_k^{(l)} = \rho_{blk}^{(l-1)} (F_k^{(l)} H_k - 1) \tag{3.13}$$

for the FB filter, where γ represents the SNR, κ is a normalized constant value that ensures the condition $\frac{1}{N}\sum_{k=0}^{N-1} F_k^{(l)} H_k = 1$ and ρ_{blk} represents the correlation factor and acts as a measure of the estimated block reliability [11]:

$$\rho_{blk}^{(l-1)} = \frac{E\left[\hat{x}_n^{(l-1)} x_n\right]}{E\left[|x_n|^2\right]} = \frac{E\left[\hat{X}_k^{(l-1)} X_k\right]}{E\left[|X_k|^2\right]} \tag{3.14}$$

Replacing the transmitted TIBWB-OFDM signal, x_n, with the FF output, $\widetilde{x}_n^{(l-1)}$, a proper approximation can be achieved [11]:

$$\rho_{blk}^{(l-1)} = \frac{E\left[\hat{x}_n^{(l-1)} \widetilde{x}_n^{(l-1)}\right]}{E\left[\left|\widetilde{x}_n^{(l-1)}\right|^2\right]} \tag{3.15}$$

When the IB-DFE makes a decision, either a *soft* or a *hard* one, it must ensure that the produced estimated block is the best possible [3]. A *hard decision* follows the minimal distance criteria and its computation is quite simple considering that it is based on the smallest possible distance between the estimated symbol and its constellation symbol. Despite of being a bit more complex, *soft* decisions significantly enhance the IB-DFE efficiency.

Rather than using a *block-wise* approach, the effectiveness of the IB-DFE receiver can be improved by estimating symbol by symbol, $\tilde{S}_{k_i}$. Considering a case where the initial OFDM symbols are directly computed using a QPSK constellation with Gray mapping, the LLR data based on the received $\tilde{S}_{k_i}$ symbol, can be expressed by:

$$\lambda_{ki}^{b_0} = log\left(\frac{Prob\left\{b_o = 0 | \tilde{S}_{k_i}\right\}}{Prob\left\{b_o = 1\,(Y)\,|\tilde{S}_{k_i}\right\}}\right) = \frac{4Re\left\{\tilde{S}_{k_i}\right\}}{\sigma_n^2} \tag{3.16}$$

and

$$\lambda_{ki}^{b_1} = log\left(\frac{Prob\left\{b_1 = 0 | \tilde{S}_{k_i}\right\}}{Prob\left\{b_1 = 1\,(X)\,|\tilde{S}_{k_i}\right\}}\right) = \frac{4Im\left\{\tilde{S}_{k_i}\right\}}{\sigma_n^2} \tag{3.17}$$

where b_0 is the *in-phase bit*, b_1 is the quadrature bit and σ_n^2 describes the complex noise with residual interference aggregated at the FF filter output.

As a result, the average bit values resulting from *soft* demodulation can be calculated as [17]:

$$\bar{\beta}_0 = Prob\{b_0 = 0\} - Prob\{b_0 = 1\} = tanh\left(\frac{\lambda_{ki}^{b_0}}{2}\right) \tag{3.18}$$

and

$$\bar{\beta}_1 = Prob\{b_1 = 0\} - Prob\{b_1 = 1\} = tanh\left(\frac{\lambda_{ki}^{b_1}}{2}\right) \tag{3.19}$$

and so, the reliability of such average bits is given by:

$$\rho_{ki}^{b_0} = \left|\bar{\beta}_0\right| = tanh\left(\frac{\left|\lambda_{k_i}^{b_0}\right|}{2}\right) \tag{3.20}$$

and

$$\rho_{ki}^{b_1} = \left|\bar{\beta}_0\right| = tanh\left(\frac{\left|\lambda_{k_i}^{b_1}\right|}{2}\right) \tag{3.21}$$

Hence, the block-wise soft reliability factor,$\tilde{\rho}_{blk}$ is determined by:

$$\tilde{\rho}_{blk} = \frac{1}{2}\sum_{i=1}^{N_S}\sum_{k=0}^{N-1}\left(\rho_{k_i}^{b_0} + \rho_{k_i}^{b_1}\right) \tag{3.22}$$

In order to accurately calculate a steady estimation for LLR and ρ_{blk}, a precise σ_η^2 estimation must a fundamental aspect in the IB-DFE receiver. In TIBWB-OFDM, the variance is estimated, based on the average SNR,γ, along with the signal bandwith [17]. Hence, σ_η^2 is indicated by:

$$\sigma_\eta^2 = \frac{\varepsilon_s}{N_x}\sum_{k=0}^{N_x-1}\frac{1}{1+\gamma|H_k|^2} \tag{3.23}$$

with ε_s being the transmitted power by each modulated symbol.

4

Time Interleaved Block Windowed Burst OFDM with Windowing Time Overlapping

Contents

TIBWB-OFDM implementation has several advantages over the conventional OFDM and BWB-OFDM, while using similar low complex systems. Although, it is still possible to increase the TIBWB-OFDM transmitter spectral efficiency, by partially overlapping the windowed OFDM blocks that compose the TIBWB-OFDM symbols. However, this leads to the need of a more sophisticated equalizer on the receiver side, since the overlapped data is corrupted before even being transmitted. Hence, a balance, between such complexity and an adequate behaviour of the system, is required [**?**, **?**].

As stated in Chapter 3, the introduction of the guard interval ZP, instead of the conventional CP, enhances the power efficiency of the scheme. The SRRC window also improves the overall performance of the system, considering it confines the spectrum and reduces the OOB emissions, when increasing the window roll-off, β. On the other hand, the length of the TIBWB-OFDM block also increases as β increases, since $N_s N_{symb} = N_s N(1+\beta)$. As a result, the spectral efficiency is limited, due to the fact that the symbol rate has to decrease. Additionally, the windowing process reduces the overall average power of the transmitted TIBWB-OFDM signal, thus limiting the PAPR reduction efficiency gains [4].

To overcome these concerns, an alternative TIBWB-OFDM packing solution was proposed and it is presented in the following section, the TIBWB-OFDM with Windowing Time Overlapping (WTO), where the windowed OFDM symbols are able to be partial overlapped.

4.1 TIBWB-OFDM Transmitter with WTO

The fundamental objective of the overlapping operation is to avoid the temporal expansion of the TIBWB-OFDM signal, induced by window roll-off factor, β. The transmission of the TIBWB-OFDM Block with WTO is similar to the one described in Section 3.2, up until the windowing of the OFDM symbols and the sub-consequently removal of its tailing zeros. At this instance, the overlapping process occurs, where each OFDM symbol are overlapped to the adjacent sub-symbols, that is, the last j samples of a given frame are added to the first samples of next frame. The TIBWB-OFDM with WTO partially overlap the tails of the OFDM symbols, which can be expressed by:

$$s_{w_0}[n] = \sum_{i=1}^{N_s} s_{w_i}[n-(i-1)N_l] \tag{4.1}$$

where $N \leq N_l \leq N_{Symb}$ and N_l addresses the first overlapped sample from each frame.

This new waveform can also be obtained by the product of the TIBWB-OFDM mega block and the overlapping matrix structure, G_0 specified in figure 4.1, with vector s_{w0} given by:

$$\mathbf{s_{w0}} = \mathbf{s_w G_0} \tag{4.2}$$

This matrix is composed by N_s identity matrices denoted by $\mathbb{I}_{N_{symb}}$. For a better understanding of how G_0 varies, the higher the desired overlapped samples, the lesser columns the matrix

has. For instance, if no overlap occurs, G_0 is square matrix with dimension $[N_s N_{symb} \times N_s N_{symb}]$.

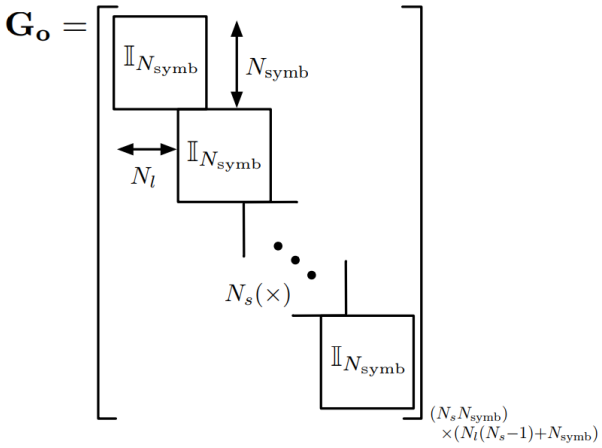

Figure 4.1: Matrix arrangement for time overlapping samples, G_0 [4]

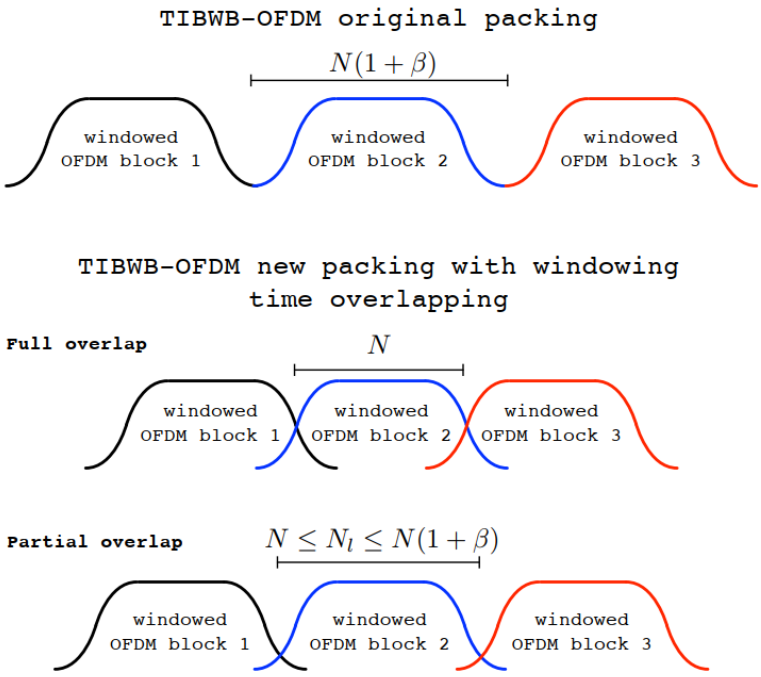

Figure 4.2: Comparison between the original TIBWB-OFDM packing method and the overlapping one (TIBWB-OFDM WTO) [4]

Figure 4.2 depicts the overlap process in a more straightforward manner, where the new total length of the block, instead of being $N_s N_{symb}$ is now $N_{OB} = N_l(N_s - 1) + N_{symb}$, with N_l being the first overlapped sample from each block. If $N_l = N$, then the block reaches its minimum possible length, $N_{block} = N(N_s + \beta)$, since the tails of the windowed symbols are

fully overlapped. This means that there is no temporal extension, when comparing with the conventional OFDM symbol packing with the rectangular window. Additionally, by using the TIBWB-OFDM packing method, the system's power efficiency has a significant increase, due to the considerable reduction of the block's PAPR. The spectrum of this new waveform can be computed as :

$$S_{wo}(e^{jw}) = \sum_{i=1}^{N_s} S_{w_i}(e^{jw}) e^{-jw(i-1)N_l} \tag{4.3}$$

4.2 TIBWB-OFDM Receiver with WTO

The TIBWB-OFDM with WTO transmitter does indeed provide significant improvement in both the spectral and power efficiencies. However, the overlapped information induces interference between adjacent sub-blocks, giving the receiver the crucial task of correctly estimate the original data. Hence, its design must enclose both a FDE and Time Domain Equalizer (TDE) in order to deal with this issue. Figures 4.3 and 4.4 depict both the transmitter and receiver scheme for the TIBWB-OFDM with WTO, respectively:

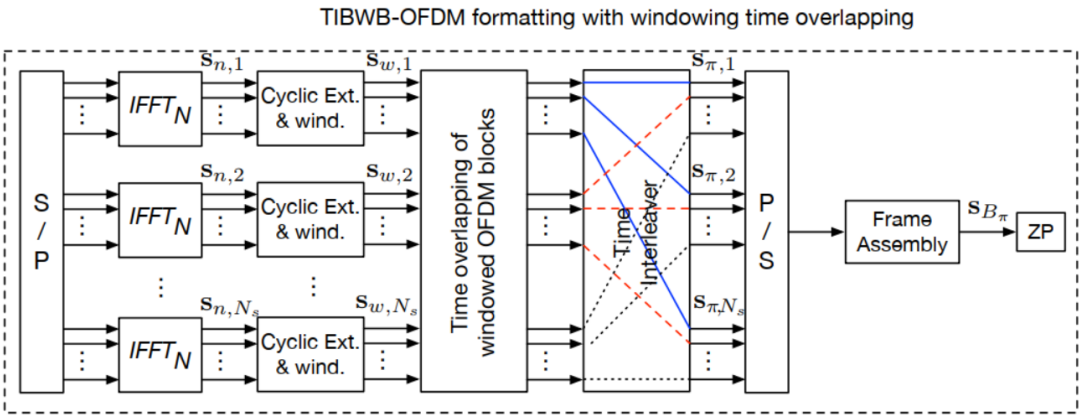

Figure 4.3: TIBWB-OFDM with WTO transmitter design [4]

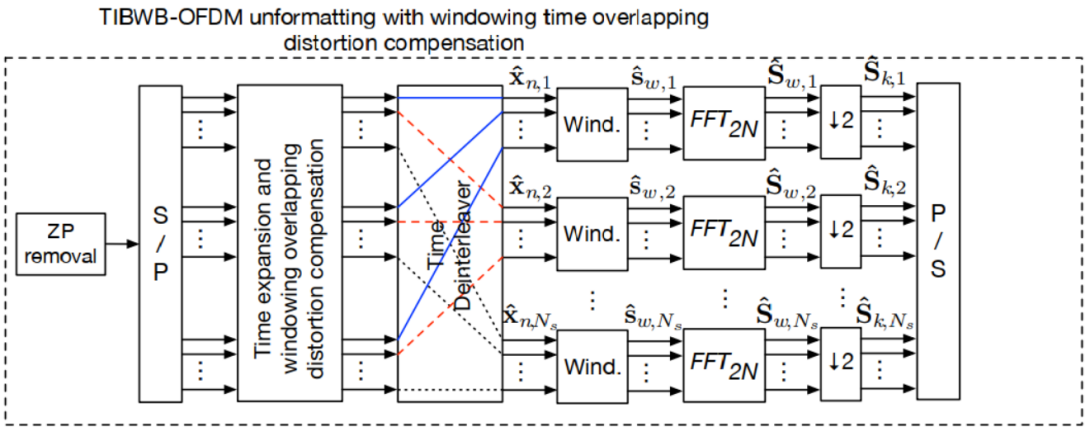

Figure 4.4: TIBWB-OFDM with WTO receiver design [4]

4.2.1 Frequency Domain Equalization

Upon reception, the TIBWB-OFDM signal can be perceived as SC block based transmission type, since TIBWB-OFDM is a hybrid modulation technique. Hence, the equalization is handled in the frequency domain, which allows the use of Frequency Domain Equalization (FDE), granting a low complexity system with relatively high robustness against channels with high delay spreads [13]. Bearing in mind that the ZP added to the original signal has to be longer than the channel's impulse response, the received signal, Y_k, at each sub-carrier $K = 0, ..., N_x - 1$ is given by:

$$Y_k = S_k H_k + \eta_k \tag{4.4}$$

where H_k is the channel's frequency response, η_k the complex addtive white Gaussian noise (AWGN) and $N_x = N_{ZP} + N_{OB}$, with N_{OB} referring as the length of the TIBWB-OFDM with WTO block.

Afterwards, an estimation of the transmitted signal, $\hat{S}_k, k = 0, ..., N_x - 1$, can be obtained by using, for instance, the IB-DFE method depicted in Section 3.3. An N_x sized IFFT is applied to the estimated signal, converting it to the time domain, and its ZP is removed. Lastly, the time deinterleaving process occurs, which shifts each symbol back to its original position.

4.2.2 Time Domain Equalizer

The FDE process provides an estimation of the TIBWB-OFDM signal that still has overlapping samples. Thus, it is necessary to cancel the "corrupted" data and obtain an estimation of the original transmitted signal, using some time domain equalization algorithm. To accurately detect the OFDM component blocks, it is fundamental to restore the length of the windowed OFDM blocks, by adding N_{zb} zeros to each symbol until it reaches a length of $2N$, so that the matched filtering operation is possible (using the same window described in 3.1). This whole procedure can be perceived as the reverse of the TIBWB-OFDM transmitter (3.6).

In this case, the product of the window and the signal is performed twice, one time on the transmitter and another on the receiver side. Therefore, the channel can be seen as the product of both of those windows, that is, its square, where $h_{RRC}[n] = h^2_{SRRC}[n]$. As illustrated by Figure 4.5, at each symbol a cyclic extension is applied, making it possible to employ the cancellation method. The forward and backward cancellation method uses the high and low amplitude parts of the adjacent OFDM blocks to successively cancel the WTO distortion they have with each other, as depicted by figure 4.6.

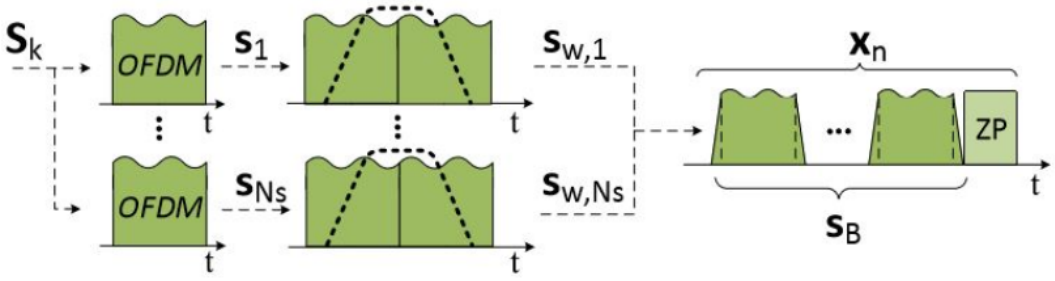

Figure 4.5: Windowing and cyclic extension of the OFDM symbols, S_k [5]

The i-th OFDM symbol, previously cyclic extended and windowed is expressed by:

$$\mathbf{s}_{w_i} = [s_{0_i}h_{-Y}, s_{1_i}h_{-Y+1}, ..., s_{Y-1_i}h_{-1}, s_{Y_i}h_0, s_{Y+1_i}h_1, ..., s_{N_{symb}-1}, h_{Y-1}] \tag{4.5}$$

where h is the SRRC window defined in (3.1), $X = \frac{N_l}{N}\frac{N}{2}(1-\beta)$ and $Y = \frac{N}{2}(1+\beta)$.

After applying the WTO at the transmitter, the symbol can be described as:

$$\begin{aligned}\mathbf{s}_{wo_i} &= [s_{wo_{i,-Y}}, s_{wo_{i,-Y+1}}, \cdots, s_{wo_{i,-1}} s_{wo_{i,0}} s_{wo_{i,1}}, \cdots, s_{wo_{i,Y-1}}] \\ &= [s_{0_i}h_{-Y} + s_{N_{l_{i-1}}}h_X, \cdots, s_{Y-1_i}h_{-1},\ s_{Y_i}h_0, \cdots, \\ &\quad s_{N_{l_i}}h_X + s_{0_{i+1}}h_{-Y}, \cdots, \\ &\quad s_{N_{symb}-1_i}h_{Y-1} + s_{N_{\text{symb}}-N_{l_{i+1}}}h_{-X}]\end{aligned} \tag{4.6}$$

4.2.3 Zero-Forcing Cancellation method

The ZF method consists in simply reverting the channel response. It is usually applied in the FDE of MC signals subject to frequency selective fading. In this case the FF filter employed at the receiver is:

$$F_k = \frac{H_k^*}{|H_k|^2}, k = 0, ..., N-1 \tag{4.7}$$

where H_k^* is the conjugate of H_k. Replacing F_k in (4.4), the estimated signal is given by:

$$\hat{S}_k = \frac{S_k H_k}{H_k} + \frac{\eta_k}{H_k} = S_k + \frac{\eta_k}{H_k} \tag{4.8}$$

ZF is ideal for a noise-free scenario, since all the data can be perfectly retrieved. Nevertheless, this method shows high noise levels in cases where the carriers suffer deep fading, inducing the channels frequency response to zero, $H_k \to 0$.

The same ZF principle can be used in time domain to compensate for the distortion caused by WTO. In the TIBWB-OFDM with WTO technique, some of the adjacent symbols are corrupted by the tails of both the previous and next symbol. Considering $\hat{\mathbf{s}}_{w1}$ and $\hat{\mathbf{s}}_{w2}$ as the vectors of the first and second windowed and cyclic extended symbols, respectively, in a noise-free situation [4]:

$$\begin{aligned}\hat{\mathbf{s}}_{wo_1} &= [\hat{s}_{w_{1,-Y}}\hat{s}_{w_{1,-Y+1}},\cdots,\hat{s}_{w_{1,-1}}\hat{s}_{w_{1,0}}\hat{s}_{w_{1,1}},\cdots,\hat{s}_{w_{1,Y-1}}] \\ &= [s_{0_1}h_{-Y}^2,\cdots,s_{Y-1_1}h_{-1}^2,\ s_{Y_1}h_0^2,\cdots, \\ &\quad s_{N_{l_1}}h_X^2 + s_{0_2}h_X h_{-Y},\cdots, \\ &\quad s_{N_{symb}-1_1}h_{Y-1}^2 + s_{N_{\text{symb}}-N_{l_2}}h_{Y-1}h_{-X}]\end{aligned} \tag{4.9}$$

$$\begin{aligned}\hat{\mathbf{s}}_{wo_2} &= [\hat{s}_{w_{2,-Y}}\hat{s}_{w_{2,-Y+1}},\cdots,\hat{s}_{w_{2,-1}}\hat{s}_{w_{2,0}}\hat{s}_{w_{2,1}},\cdots,\hat{s}_{w_{2,Y-1}}] \\ &= [s_{0_2}h_{-Y}^2 + s_{N_{l_1}}h_X h_{-Y},\cdots,s_{Y-1_2}h_{-1}^2,\ s_{Y_2}h_0^2,\cdots, \\ &\quad s_{N_{l_2}}h_X^2 + s_{0_3}h_X h_{-Y},\cdots, \\ &\quad s_{N_{symb}-1_2}h_{Y-1}^2 + s_{N_{\text{symb}}-N_{l_3}}h_{Y-1}h_{-X}]\end{aligned} \tag{4.10}$$

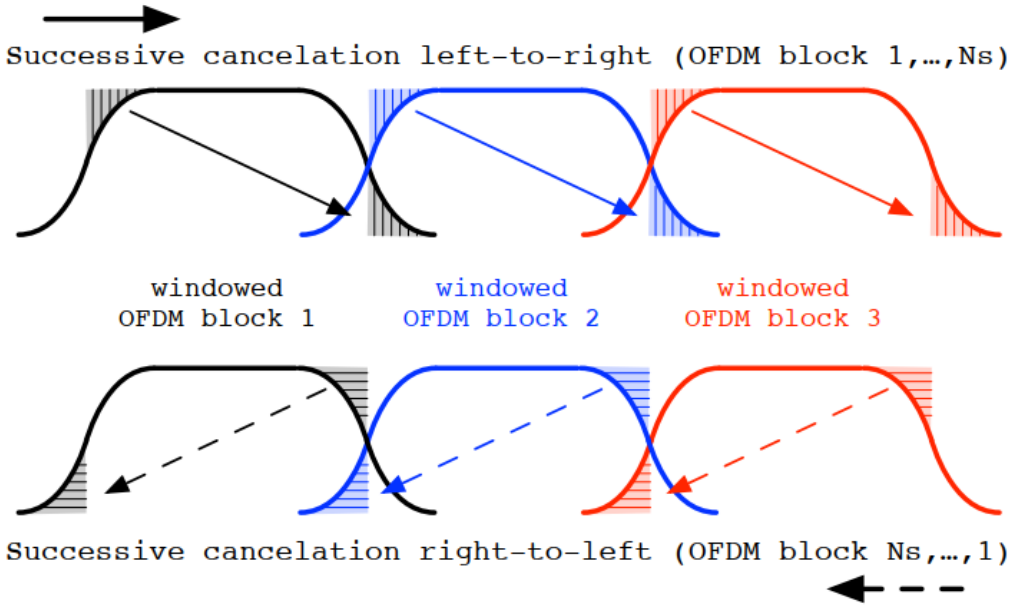

Figure 4.6: Forward and backward successive interference cancellation model [6]

As perceived by Figure 4.6, where the principles of the forward and backward sucessive interference cancellation are depicted, both the left tail and the right tail of the OFDM block of

the TIBWB-OFDM symbol present no interference whatsoever. Thus, allied to the knowledge of the SRRC window influence [6], it is possible to correctly estimate the interference in the second symbol, caused by the first one (forward direction), and in symbol $N_s - 1$ due to the last one (backward direction). Applying Hadamard multiplication and division to the left tail of the first symbol produces an estimation of the information sent on the right tail of that symbol, which is interfering with the left tail of the second symbol. This way, it is possible to obtain the original sent data at the second symbol, by subtracting the left tail of the first symbol to the samples from the left tail of the second symbol.

Considering $\hat{s}_{w_2,j}$ as the corrupted samples of the second symbol, the original samples can be retrieved following:

$$\hat{s}^I_{w_2,j} = \hat{s}_{w_2,j} - h^2_{(j+N_l)} \frac{\hat{s}_{w_1,j}}{h^2_j} \tag{4.11}$$

where $j = -\frac{N}{2}, \cdots, -\frac{N}{2}(1-\beta)$. This operation can be extended to a general case for a symbol i, as so:

$$\hat{s}^I_{w_i,j} = \hat{s}_{w_i,j} - h^2_{(j+N_l)} \frac{\hat{s}_{w_i-1,j}}{h^2_j} \tag{4.12}$$

with $i = 1, \cdots, N_s$.

The backward cancellation follows and identical pattern, where $j = \frac{N}{2}(1-\beta), \cdots, \frac{N}{2}$, starting on the left tail of the last symbol. The right of this symbol has no interference, so it is similar to the left tail of the first symbol. Hence, it is also possible to get an estimation of the interference created by the last symbol in its precent symbol.

4.2.4 Minimum Mean Square Error (MMSE) Cancellation method

Given that the ZF approach struggles in poor channel conditions, the MMSE true to overcome channel deep fades. Thereby, this method's main goal is to minimize the square error, $\left\{E\left[\hat{S}_k - S_k\right]\right\}, k = 0, \ldots, N-1,$, which translates to:

$$F_k = \frac{H^*_k}{|H_k|^2 + \frac{1}{\gamma}} \tag{4.13}$$

where γ represents the Signal-to-Noise Ratio (SNR). Thus, the estimated signal can be expressed by:

$$\hat{S}_k = \frac{S_k H_k H^*_k}{|H_k|^2 + \frac{1}{\gamma}} + \frac{\eta_k H^*_k}{|H_k|^2 + \frac{1}{\gamma}} = \frac{S_k |H_k|^2}{|H_k|^2 + \frac{1}{\gamma}} + \frac{\eta_k H^*_k}{|H_k|^2 + \frac{1}{\gamma}}. \tag{4.14}$$

From this equation (4.14), it is easy to aknowledge that, for low SNR values, the noise enhancing problem is worked out and for high SNR values the MMSE acts like a ZF equalizer.

While applying the MMSE method to WTO schemes, the forward and backward cancellation (4.6) is expressed by:

$$\hat{s}^{I}_{w_i,j} = \hat{s}_{w_i,j} - h^2_{(j+N_l)}\hat{s}_{w_i-1,j}\frac{h_j^2}{\left(h_j^2\right)^2 + \frac{1}{\gamma}} \tag{4.15}$$

where the Hadamard division is only performed at the end using the SNR value.

4.3 TIBWB-OFDM with matrix approach

In this section it is proposed an efficient matrix based implementation of the TIBWB-OFDM transceiver with WTO.

As seen throughout the previous sections, the TIBWB-OFDM transceiver was largely expanded until reaching a peak of its spectral and power efficiency, by using proper packing, windowing and equalization methods. The use of a smoother SRRC window (3.1) grants a higher spectrum confinement of the transmitted OFDM symbols, while keeping the same symbol energy as the OFDM. Additionally, the WTO process allows a considerable reduction in the total length of the packed OFDM symbols, which also improves transmission rate, when comparing with the conventional windowed OFDM.

4.3.1 TIBWB-OFDM Transmitter with matrix approach

Furthermore, the TIBWB-OFDM transmitter can take a matrix approach. For instance, instead of windowing an OFDM block and then remove its trailing and ending zeros, the matrix approach proposes to process these operations all at once. This means that, after studying the behaviour of the system, the desired matrices are precomputed, allowing a lower complexity scheme.

Hence, the main concept is to compact the Formatting, Filtering and Fourier Analysis processes into matrix operations. Considering $\mathbf{S}_i = \left[S_{i,0}, S_{i,1}, \cdots, S_{i,(N-1)}\right]^T$ as the i-th N-carrier OFDM symbol, where $i = 0, \cdots, N_{s-1}$ and $\mathbf{S} = \left[\mathbf{S}_0, \mathbf{S}_1, \cdots, \mathbf{S}_{N_{s-1}}\right]$ and $\mathbf{F^{-1}}$ as the Inverse Discrete Fourier Transform (IDFT) square matrix $(N \times N)$ that converts the symbol stream into the time domain, the N_s OFDM symbols can be expressed by:

$$\mathbf{F^{-1}S} = \begin{bmatrix}\mathbf{s}_0 & \mathbf{s}_1 & \cdots & \mathbf{s}_{N_{s-1}}\end{bmatrix}_{(N \times N_s)} \tag{4.16}$$

A cyclic extension must be employed to each of those N_s symbols, before applying the windowing process:

$$\mathbf{1}_2 \otimes \mathbf{F^{-1}S} = \begin{bmatrix}\mathbf{s}_0 & \mathbf{s}_1 & \cdots & \mathbf{s}_{N_{s-1}} \\ \mathbf{s}_0 & \mathbf{s}_1 & \cdots & \mathbf{s}_{N_{s-1}}\end{bmatrix}_{(2N \times N_s)} \tag{4.17}$$

where $\mathbf{1_l}$ represents a l-sized vector of 1s and $\otimes$ the Kronecker multiplication.

Let $\mathbf{h}_{SRRC} = \begin{bmatrix} 0, & h_{SRRC_{-N}}, & \cdots, & h_{SRRC_0}, & \cdots, & h_{SRRC_N}, & 0 \end{bmatrix}^T_{(2N \times N_s)}$ be the vector of SRRC coefficients with length $2N$. The windowing operation can then be performed as:

$$\mathbf{1}^T_{N_s} \otimes \mathbf{h}_{SRRC} \tag{4.18}$$

The BWB-OFDM block, as defined in 3.3, can thus be matritially computed as:

$$\mathbf{s}_B = \begin{bmatrix} s_{w_0}, & s_{w_1}, & \cdots, & s_{N_{s-1}} \end{bmatrix} = \mathbf{A}\left(\mathbf{1}^T_{N_s} \otimes \mathbf{h}_{SRRC}\right) \odot \left(\mathbf{1}_2 \otimes \mathbf{F^{-1}S}\right) \tag{4.19}$$

where $\odot$ represents the point-wise Hadamard multiplication and $\mathbf{A}$ depicts a matrix that cuts out the trailing and ending lines of zeros created by the SRRC windowing process and can be written as:

$$\mathbf{A} = \begin{bmatrix} \mathbf{0}_{N(1+\beta)} & \mathbf{I}_{N(1-\beta)} & \mathbf{0}_{N(1+\beta)\times\frac{N}{2}(1-\beta)} \end{bmatrix} \tag{4.20}$$

$\mathbf{I}_n$ is an identity $(n \times n)$-size matrix and $\mathbf{0}_{m\times n}$ is a $(m \times n)$-sized matrix of zeros.

Lastly, the windowed symbols are juxtaposed and time-interleaved, increasing the robustness against the deep-in band fades [3], generating the TIBWB-OFDM block (3.6):

$$\mathbf{s}_\pi = \Pi^{(N_s)} vect(\mathbf{s_B}) \tag{4.21}$$

where $\Pi^{(N_s)}$ is the permutation square N_s-sized matrix that performs the time-interleaving process, with period N_s and $vect()$ is a vector which mutates a matrix into a column (through column reading).

The matrix approach used for building the TIBWB-OFDM with WTO block, $\mathbf{X}$, follows a similar approach and it is given by:

$$\mathbf{X} = \Pi^{(N_s)} vect\left[\mathbf{A}\left(\left(\mathbf{1}^T_{N_s} \otimes \mathbf{h}_{SRRC}\right) \odot \left(\mathbf{1}_2 \otimes \mathbf{F^{-1}S}\right)\right)\mathbf{G_0}\right] \tag{4.22}$$

where $\mathbf{G_0}$ is the overlap matrix mentioned in Figure 4.1.

Reminding that the overall TIBWB-OFDM symbol construction process remains the same as stated in Section 3.6, after $\mathbf{X}$ is computed, a ZP, longer than the channel's delay spread, is added at the end of each block, granting robustness to ISI. Thus, the TIBWB-OFDM with WTO blocks are ready to be obtained and equalized by the receiver.

4.3.2 Matrix framework for the TIBWB-OFDM Receiver

The TIBWB-OFDM receiver has the crucial task to correctly estimate and equalize the TIBWB-OFDM with WTO block (4.2). Hence, upon reception, the ZP guard interval is removed the TIBWB-OFDM block y and the time-deinterleave operation is performed:

$$y_\pi = \Pi^{T(N_s)} vect(y) \tag{4.23}$$

where $\Pi^{T(N_s)}$ is the permutation square N_s-sized matrix that performs time-deinterleaving, that is, the transpose matrix of $\Pi^{(N_s)}$, and $vect()$ is a vector that mutates a matrix into a column. The minimum length of the block, in a fully overlapped scenario, is $N_l(N_s+\beta)$. If no overlap occurs the block has length equal to $N_s N_{symb}$.

Considering a noiseless transmission, the signal's equalization can be easily performed by a ZF equalizer. Based on the fact that the windowing factors of the employed SRRC window on the overall TIBWB-OFDM block are fully known, it is possible to entirely estimate the interference caused by the overlapped samples. Hence, a conceivable approach to this problem is to build a matrix that, when applied to TIBWB-OFDM block with WTO, both unfolds the overlap process and achieves matched-filtering. However, for better understanding, these will be addressed as separated matrices operations. The interference compensation, caused by WTO, is achievable relying on the principle of the forward and backward successive interference cancellation, stated in 4.6, where the $\frac{N}{2}\beta+1$ higher coefficients of the left tail of the windowed symbol, h_{left}, can correlate with the ones on the right tail, h_{right}, resulting in the windowing influence factors, $a=-\frac{h_{right}}{h_{left}}$. The *De-overlap* matrix, $\mathbf{D_0}$, is a $(N\times N_s)$-sized matrix and its architecture is described in Figure 4.7.

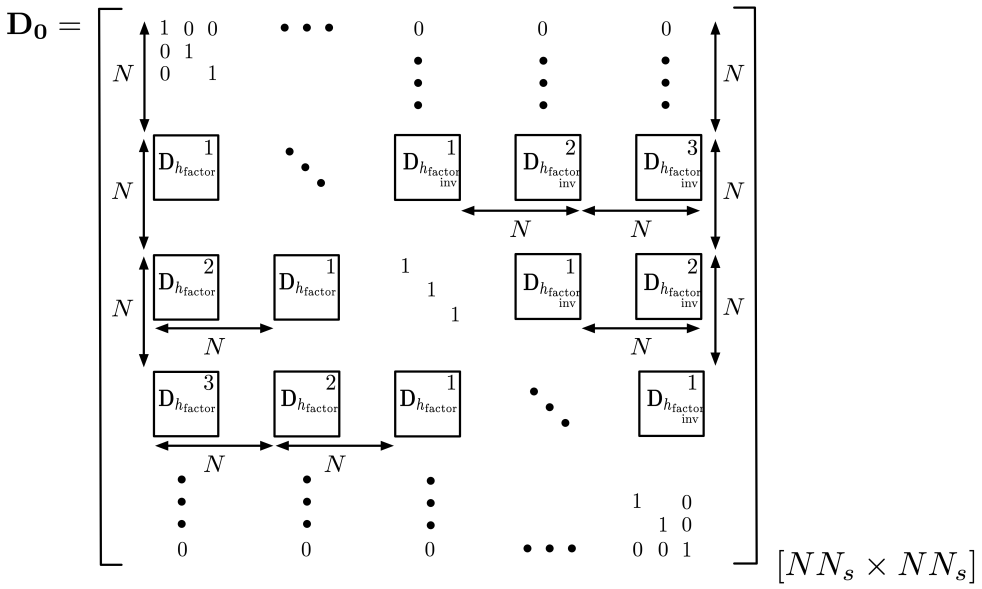

Figure 4.7: Square $(NN_s\times NN_s)$-sized matrix design, D_0, for time de-overlapping samples, when the transmitted symbols are fully overlapped (4.1).

$\mathbf{D}_{h_{factor}}^{i-j}$ represents the $\left(\frac{N}{2}\beta+1\right)$-sized diagonal square matrix that cancels the interference on windowed symbol i due to symbol $i-j$, with $i=0,\cdots,N_s-1$ and $j=0,\cdots,i-1$, where $\mathbf{D}_{h_{factor}}$ is given by:[1]:

[1]Note that, since unfolding and interference compensation due to WTO is carried separated and prior to match-filtering, the ZF coefficients as defined in (4.11) and (4.12) do not come squared.

$$\mathbf{D}_{h_{\text{factor}}} = \begin{bmatrix} -\frac{h_{-\frac{N}{2}\beta+N_l}}{h_{\frac{N}{2}\beta}} & 0 & 0 & \cdots & 0 \\ 0 & -\frac{h_{-\frac{N}{2}\beta+1+N_l}}{h_{\frac{N}{2}\beta+1}} & & & 0 \\ \vdots & & -\frac{h_{-\frac{N}{2}\beta+2+N_l}}{h_{\frac{N}{2}\beta+2}} & \ddots & \vdots \\ 0 & 0 & 0 & \cdots & -\frac{h_{0+N_l}}{h_0} \end{bmatrix}_{\left[\left(\frac{N}{2}\beta+1\right)\times\left(\frac{N}{2}\beta+1\right)\right]}$$

Figure 4.8: Diagonal square $\left(\frac{N}{2}\beta+1\right)$-sized matrix that contains the windowing factors, h_k

The indexes, $1,2,3,\cdots,N_s-1$, present inside the $\mathbf{D}_{h_{factor}}$ matrix on Figure 4.7 can be seen as $\mathbf{D}^N_{h_{factor}}$, i.e the power of the matrix $\mathbf{D}_{h_{factor}}$, where the exponent is of N power.

In fact, D_0 resembles the implementation of the forward and backward successive interference cancellation method, illustrated in Figure 4.6 and detailed in (4.9) and (4.10), where the lower triangular part of the matrix represents the forward cancellation and the upper triangular part features the backward cancellation. Considering a TIBWB-OFDM block, with 3 symbols, as depicted in the mentioned figure, $\hat{s}_{w_1,j}$, $\hat{s}_{w_2,j}$ as the interference of the symbols and let $\hat{s}_{wo_{i,j}}$ denote received samples associated to the i-th OFDM block of the received TIBWB-OFDM with WTO symbol. The estimated symbol can be expressed by:

$$\hat{s}_{w_1,j} = \hat{s}_{wo_1,j} - h_{(j+N_l)}\frac{\hat{s}_{0,j}}{h_j} \tag{4.24}$$

$$\hat{s}_{w_2,j} = \hat{s}_{wo_{2,j}} - \frac{h_{(j+N_l)}}{h_j}\hat{s}_{w_1,j} = \hat{s}_{wo_{2,j}} - \frac{h_{(j+N_l)}}{h_j}\hat{s}_{wo_1,j} + \frac{h^2_{(j+N_l)}}{h^2_j}s_{wo_{0,j}} \tag{4.25}$$

This cancellation method is possible due to $\mathbf{D}_{h_{factor}}$, since it provides the windowing factors to perfectly estimate the existent interference, as the left tail of the received signal is free of any interference from its later symbol [4]. The backward successive cancellation method process follows an identical approach, starting at the end of the TIBWB-OFDM block and using the diagonally inverted $\mathbf{D}_{h_{factor}}$.

So, as the left and right tails of the fully overlapped TIBWB-OFDM block, have no influence in the overlap process, $\frac{N}{2}\beta$ samples are removed from each extremity. This way, the product between the TIBWB-OFDM block (y_π) without its tails, y_w, and the square NN_S-sized $\mathbf{D_0}$ matrix is given by:

$$\hat{\mathbf{s}}_c = y_w\mathbf{D_0} \tag{4.26}$$

where $\hat{\mathbf{s}}_c$ is the NN_s-sized column-wise vector that represents the *de-overlapped* TIBWB-OFDM compensated block. However, it is still necessary to properly expand the signal into its original

transmitted dimensions, $2N \times N_s$ (including the trailing zeros caused by the windowing operation), by both unfolding the interferences and perform match-filtering. Thus, $\hat{\mathbf{s}}_c$ is rearranged into a $N \times N_s$-sized matrix, representing each tailless OFDM symbol $(1, 2, \cdots, N_s)$ like so:

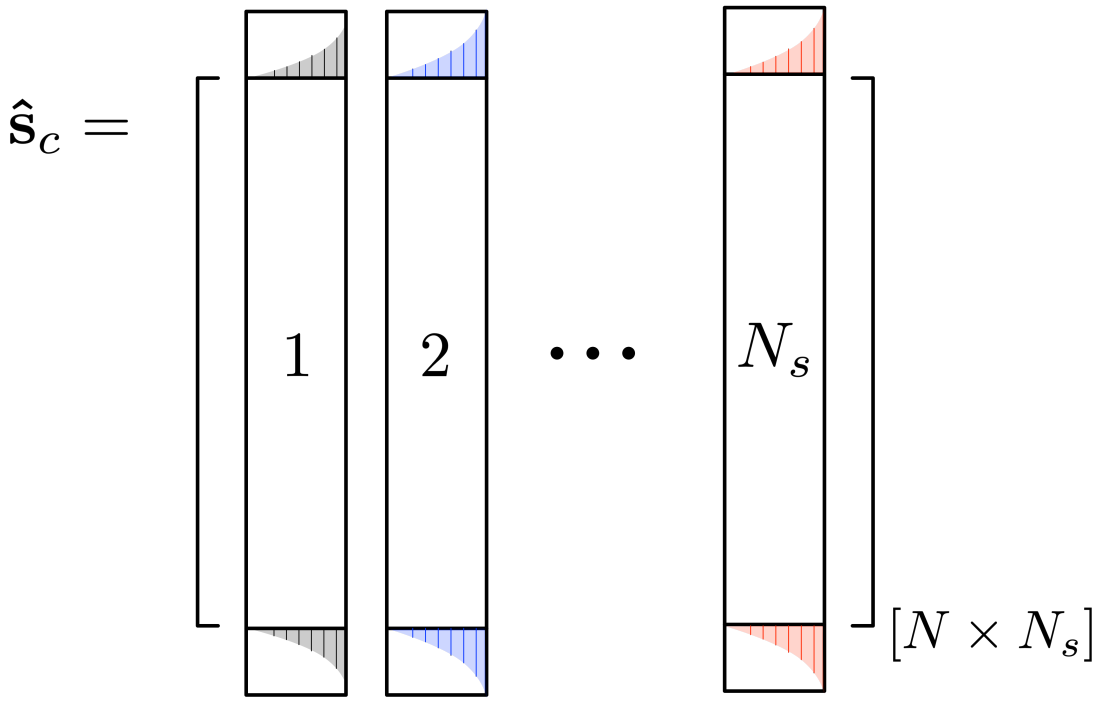

Figure 4.9: Tailless compensated TIBWB-OFDM $N \times N_s$-sized block composed of N_s N-sized OFDM symbols, $\hat{\mathbf{s}}_c$.

The scratched coloured parts of the Figure display the $\frac{N}{2}\beta$-sized tails that need to be added back on each N-sized OFDM symbol. Since a noiseless transmission was assumed, those tails can be straightforwardly computed as they exclusively depend on the SRRC windowing factors, $-\frac{h_{-\frac{N}{2}\beta+N_l}}{h_{\frac{N}{2}\beta}}$, similarly to the process depicted in $\mathbf{D}_{h_{factor}}$ on Figure 4.8. Afterwards, a simple matrix multiplication of $\hat{\mathbf{s}}_c$ with $\mathbf{E_0}$ (Figure 4.10 - the expansion matrix) results in the $2N \times N_s$-sized TIBWB-OFDM block. The obtained symbols with the WTO interferences correctly unfolded, are then match-filtered with 4.18, resulting in:

$$\hat{\mathbf{s}}_E = (\mathbf{1}_{N_s}^T \otimes \mathbf{h}_{SRRC}) \odot (\mathbf{E_0}\hat{\mathbf{s}}_c) \tag{4.27}$$

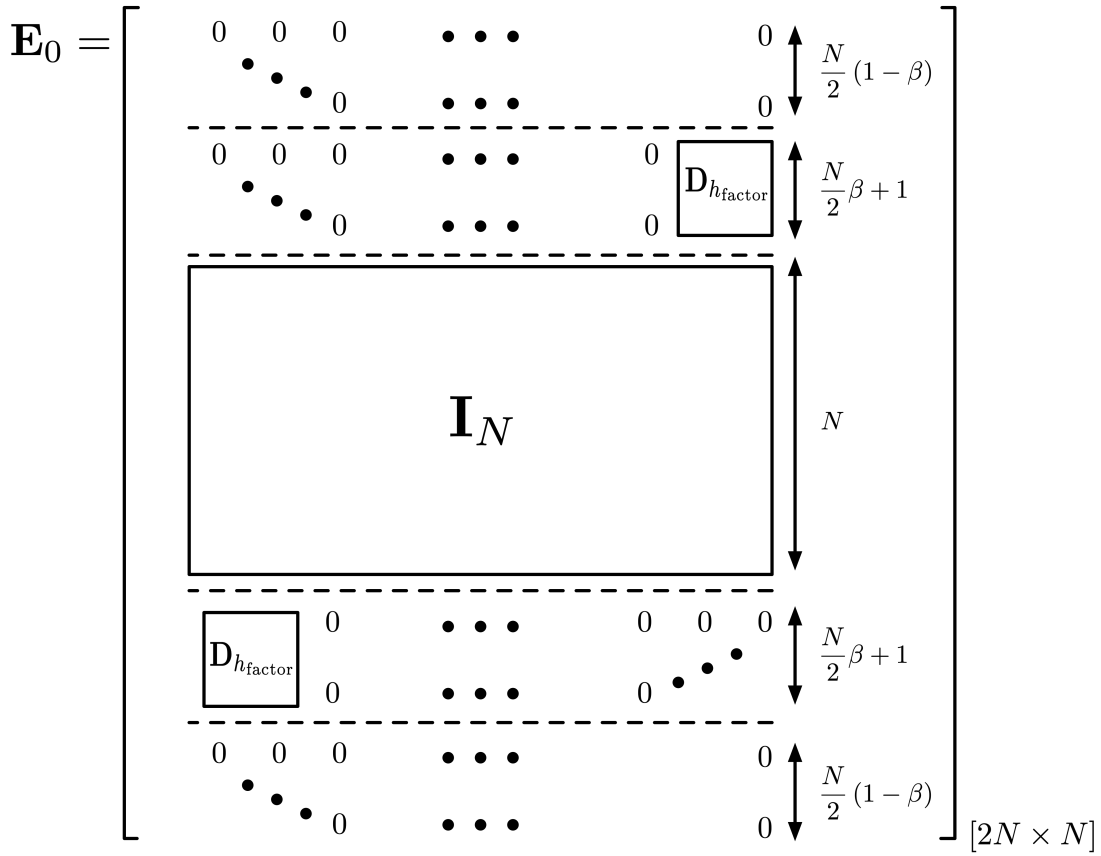

Figure 4.10: $(2N \times N)$-sized matrix, $\mathbf{E_0}$, used for expanding the overlapped symbols

The upper and lower parts of $\mathbf{E_0}$ suggest the trailing zeros, caused by the SRRC windowing process. The section containing $\mathbf{D}_{h_{factor}}$ indicates the windowing factors that compensate and add both the left and right tails to each symbol, respectively, performing the matched-filtering operation. The center of $\mathbf{E_0}$ is an identity $N \times N$ matrix ($\mathbf{I_N}$), since the intermediate samples of the OFDM symbols are not affected by the WTO process, remaining unchanged.

The resulting TIBWB-OFDM block, $\hat{\mathbf{s}}_E$, is then unformatted according to the conventional TIBWB-OFDM receiver, as represented in Figure 3.7.

In summary, $\hat{\mathbf{s}}_E$ is deinterleaved, obtaining the time domain OFDM blocks, $\hat{\mathbf{x}}_{n,i}$ with $i = 1, \cdots, N_s$ followed by a $2N$-sized FFT, decimation by 2 and demodulation into the original $2N \times N_s$-sized transmitted bit-stream.

This new implementation allows an efficient and fast computation, as both the *De-overlap* matrix ($\mathbf{D_0}$) and the expansion matrix ($\mathbf{E_0}$), although having a considerable size, are very sparse matrices. This means that they have a large number of zero-valued elements, which saves a huge amount of memory, as well as granting a higher speed processing. Furthermore, the matrix approach grants a possible parallelization of the TIBWB-OFDM transceiver, where the high data rate transmissions and respective equalization's can be solved independently.

5

Conclusions

This dissertation proposed a matrix approach for the TIBWB-OFDM transceiver, more specifically when applying Windowing Time Overlapping. Since a noiseless scenario was considered *a priori*, the ZF equalization method was chosen to perfectly estimate the symbols interference caused by the overlapping operation.

The TIBWB-OFDM with WTO presents a more confined spectrum, by partially overlapping the adjacent symbols, achieving higher spectral efficiency values. This means that less power is required for the transmission of the block, since several samples are overlapped with eachother. However, this originates ISI, which leads to the need of more complex equalization techniques. The developed work proves that it is possible to mutate the operations associated with TIBWB-OFDM, including the equalization, into simple and straightforward matrices and thus, lower complexity systems. This way, by only defining the main variables of the TIBWB-OFDM, such as the number of OFDM sub-carriers, N, the number of BWB-OFDM symbols, N_s and the window roll-off value, β, some matrices can be pre-computed, granting an improvement in the system's computational efficiency. The implemented matrices are very sparse, meaning that the mathematical operations are processed with higher speed than the conventional TIBWB-OFDM. Additionally, by enforcing the matrix approach to the TIBWB-OFDM scheme, it is conceivable to achieve a parallelization of this modulation technique.

For future research, since this work was only performed in a noiseless and simulated environment, it should be interesting to apply the matrix framework to TIBWB-OFDM with WTO in a real-life scenario, bringing the need to develop new channel synchronization and estimation algorithms, as well as new equalization methods, in order to enhance the BER performance.

Bibliography

[1] T. Fernandes, "Time-Interleaved BWB-OFDM with Iterative FDE," no. December 2011, pp. 1–110, 2015.

[2] T. Fernandes, M. Gomes, V. Silva, and R. Dinis, "Time-Interleaved Block-Windowed Burst OFDM," *IEEE Vehicular Technology Conference*, vol. 0, 2016.

[3] T. Fernandes, "A new hybrid multicarrier transmission technique with iterative frequency domain detection," *Physical Communication*, 2018. [Online]. Available: https://doi.org/10.1016/j.phycom.2017.12.014

[4] F. Conceicao, M. Gomes, V. Silva, and R. Dinis, "Highly efficient TIBWB-OFDM waveform for broadband wireless communications," *IEEE Vehicular Technology Conference*, vol. 2020-May, 2020.

[5] Rohde & Schwarz, "5G Waveform Candidates," *White Paper*, pp. 1–60, 2016. [Online]. Available: https://www.rohde-schwarz.com/de/applikationen/application-note{_}56280-267585.html

[6] F. Conceição, "New Hybrid Modulation Techniques for Future Generations of Communications," 2019.

[7] r. G. P. P. 3GPP, "About 3GPP," p. About 3GPP, 2016. [Online]. Available: http://www.3gpp.org/about-3gpp

[8] R. Prasad, *OFDM for Wireless Communications Systems*. Artech House, 2004.

[9] A. Pereira, "Low Complexity Iterative Frequency Domain Equalisation for MIMO-OFDM Type SystemS," Ph.D. dissertation, 2016.

[10] X. Yin and X. Cheng, *Propagation Channel Characterization, Parameter Estimation, and Modeling for Wireless Communications*. Wiley-IEEE Press, 2016.

[11] T. D. Chiueh and P. Y. Tsai, "OFDM Baseband Receiver Design for Wireless Communications," *OFDM Baseband Receiver Design for Wireless Communications*, pp. 1–258, 2009.

[12] S. S. Haykin, *Digital Communication Systems*, 2014.

[13] Tarokh V., *New Directions in Wireless Communications*. Springer Publishing Company, Incorporated, 2009.

[14] H. A. Bottomley and G. E., *Wireless Communications and Mobile ComputingVolume 1*. NC: John Wiley & Sons, Ltd., 2001. [Online]. Available: https://onlinelibrary.wiley.com/doi/10.1002/wcm.14

[15] Y. R. Mohan and S., *Peak-To-Average Power Ratio Reduction in OFDM Systems: A Survey And Taxonomy*, 15th ed., I. C. Surveys and Tutorials, Eds., 2013.

[16] T. Fernandes, M. Gomes, V. Silva, and R. Dinis, "Time-Interleaved Block-Windowed Burst OFDM," *IEEE Vehicular Technology Conference*, vol. 0, 2016.

[17] X. Lin, J. Li, R. Baldemair, T. Cheng, S. Parkvall, D. Larsson, H. Koorapaty, M. Frenne, S. Falahati, A. Grövlen, and K. Werner, *5G New Radio: Unveiling the Essentials of the Next Generation Wireless Acess Technology*, CoRR, Ed., 2018.

[18] C. C. J. K. M.-o. P. M. Morelli, *Multi-Carrier Techniques For Broadband Wireless Communications: A Signal Processing Perspective*. Imperial College Press.

[19] F. Conceição, M. Gomes, V. Silva, R. Dinis, A. Silva, and D. Castanheira, "A Survey of Candidate Waveforms for beyond 5G Systems," *Electronics*, vol. 10, no. 1, p. 21, 2020.

[20] J. Manuel and C. Gil, "Time Interleaved Block Windowed Burst OFDM: Channel Estimation and Synchronization Techniques," Ph.D. dissertation, UC, 2020.

[21] F. Coelho, R. Dinis, N. Souto, and P. Montezuma, "On the impact of multipath propagation and diversity in performance of iterative block decision feedback equalizers," *2010 IEEE 6th International Conference on Wireless and Mobile Computing, Networking and Communications, WiMob'2010*, pp. 246–251, 2010.

[22] *Intersymbol Interference in Digital Communication Systems*. Wiley Online Library, 2001.

[23] P. P. V. Y.-P. L. S.-M. Phoong, *Filter Bank Transceivers for OFDM and DMT Systems*, 3rd ed. Cambridge University Press, 2011.

[24] A. Pereira, P. Bento, M. Gomes, R. Dinis, and V. Silva, "MIMO time-interleaved block windowed burst OFDM with iterative frequency domain equalization," *Proceedings of the International Symposium on Wireless Communication Systems*, vol. 2018-Augus, 2018.

[25] J. Martins, F. Conceição, M. Gomes, V. Silva, and R. Dinis, "Joint channel estimation and synchronization techniques for time-interleaved block-windowed burst OFDM," *Applied Sciences (Switzerland)*, vol. 11, no. 10, 2021.

[26] E. Hossain and M. Hasan, "5G cellular: Key enabling technologies and research challenges," *IEEE Instrumentation and Measurement Magazine*, vol. 18, no. 3, pp. 11–21, 2015.

A

Appendix I - Simulink Model

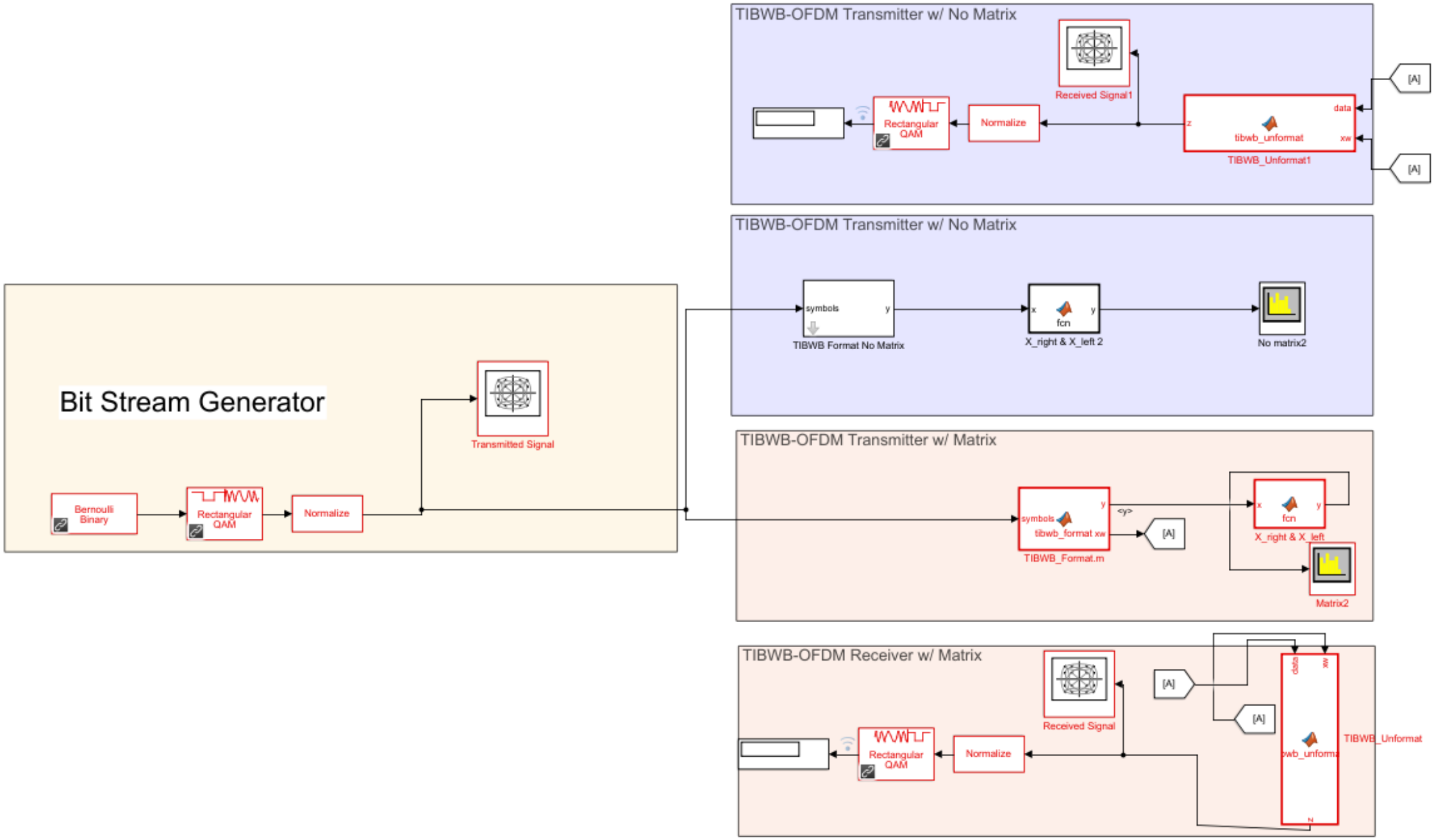
TIBWB-OFDM Transmitter w/ No Matrix
Received Signal1
Rectangular QAM
Normalize
tibwb_unformat
data
xw
TIBWB_Unformat1
[A]
[A]
TIBWB-OFDM Transmitter w/ No Matrix
symbols
y
TIBWB Format No Matrix
x
fcn
y
X_right & X_left 2
No matrix2
Bit Stream Generator
Transmitted Signal
Bernoulli Binary
Rectangular QAM
Normalize
TIBWB-OFDM Transmitter w/ Matrix
symbols
tibwb_format xw
y
<y>
TIBWB_Format.m
[A]
x
fcn
y
X_right & X_left
Matrix2
TIBWB-OFDM Receiver w/ Matrix
Received Signal
Rectangular QAM
Normalize
[A]
[A]
data
xw
TIBWB_Unformat
N